Moodley and Guardabassi, 2009; Mulvey *et al.*, 2009; Smet *et al.*, 2009; Zhang *et al.*, 2009; Jakobsen *et al.*, 2010, 2011; Zhao *et al.*, 2010; Deng *et al.*, 2011; Vieira *et al.*, 2011; Stokes *et al.*, 2012; Ciccozzi *et al.*, 2013; Hu *et al.*, 2013; de Been *et al.*, 2014; Hammerum *et al.*, 2014; Valentin *et al.*, 2014; Dahms *et al.*, 2015; Dohmen *et al.*, 2015; Huijbers *et al.*, 2015; Lupindu *et al.*, 2015; Tseng *et al.*, 2015), and 12 studies (26%) did not suggest to find evidence supporting transmission between food animals and humans (Kariuki *et al.*, 1997, 1999; Maynard *et al.*, 2004; Kang *et al.*, 2005; Phongpaichit *et al.*, 2007; Graziani *et al.*, 2009; Schwaiger *et al.*, 2010; Xia *et al.*, 2010; Johnson *et al.*, 2012; Riccobono *et al.*, 2012; Jakobsen *et al.*, 2015; Ueda *et al.*, 2015). No study in our review suggested to provide evidence for AMR transmission from humans to food animals (Fig. 3).

Only one study (2%) based its conclusion regarding transmission on high resolution typing tools, 36 studies (80%) on intermediate resolution typing tools, six (13%) on low resolution typing tools, and two (5%) on co-occurrence of resistances (Fig. 3). Overall, 18 (40%) studies based their conclusion on transmission of AMR determinants, nine (20%) on transmission of AMR bacteria, and 18 (40%) transmission of AMR bacteria together with AMR determinants (Supplementary Fig. S4 in the Supplementary Data). We found no statistical association between whether direction of transmission was inferred and the nature of transmission ($p = 0.33$).

### *Studies suggesting to provide evidence of transmission of AMR from food animals to humans with direction specified*

Three studies suggested to find evidence for transfer of AMR bacteria from food animals to humans, two of which concluded there is transfer of resistant clones from poultry to humans (Al-Ghamdi *et al.*, 1999; van den Bogaard *et al.*, 2001). In addition to overlapping clonal patterns, one study reported that human and chicken isolates were resistant to spectinomycin, an antibiotic mostly used in veterinary medicine (Al-Ghamdi *et al.*, 1999). Similarly, one study (van den Bogaard *et al.*, 2001) reported a higher prevalence of ciprofloxacin resistance among food animal isolates compared to human isolates.

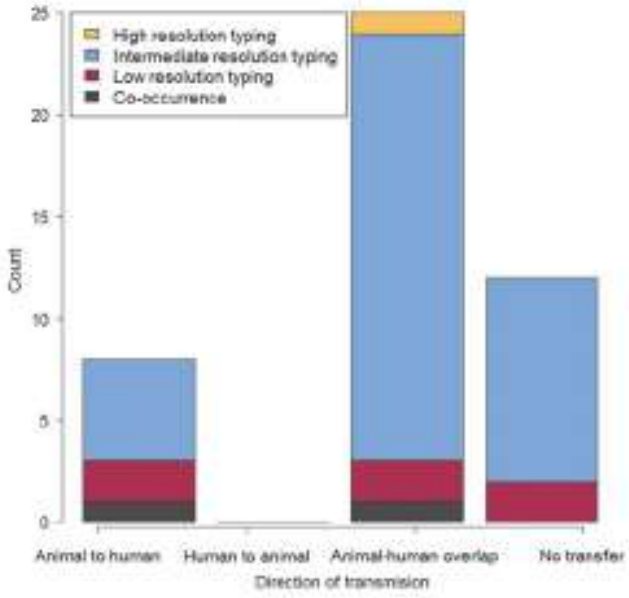


**FIG. 3.** Nature of evidence used to infer direction of transmission in each study. Color images available online at www.liebertpub.com/fpd

One study found identical ciprofloxacin-resistant isolates in chicken and humans, which they concluded was suggestive of food animal to human AMR transmission (Johnson *et al.*, 2006). Two studies suggested to find evidence for horizontal transfer of AMR determinants from food animals to humans (Hammerum *et al.*, 2006; Dierikx *et al.*, 2013). One study found that clonally unrelated poultry and human isolates shared ESBL/AmpC genes located on identical plasmid families (Dierikx *et al.*, 2013). Another study found that sulfonamide-resistant isolates from pigs and healthy humans shared sul1 and sul2 genes (Hammerum *et al.*, 2006).

Three studies suggested to support transmission of both AMR bacteria and their AMR determinants from food animals to humans. Two studies found similar sequence types, plasmid families and ESBL genes in *E. coli* isolates sourced from poultry and human patients (Leverstein-van Hall *et al.*, 2011; Giufre *et al.*, 2012). A further study reported an increase in tetracycline-resistant *E. coli* in humans in contact with tetracycline fed chicken and, therefore, suggested that chicken were a reservoir of AMR bacteria and plasmids for humans (Levy, 1978).

We found that studies suggesting to provide evidence of transmission of AMR from food animals to humans did not have distinct features compared to those suggesting overlap of resistance, with regard to study methodologies, food animal species, typing tools, or antibiotics tested. For most of these it is unclear why they suggested evidence of directional transmission when 25 broadly similar studies suggested only overlap of resistance.

### *Studies suggesting overlap indicating the possibility of between-host AMR transmission, with no direction specified*

Four studies suggested there was evidence of overlap of resistant *E. coli* between humans and food animals. One of these studies found human and avian sequence types associated with multidrug resistance clustered together in a Bayesian phylogenetic tree (Ciccozzi *et al.*, 2013). Another study found indistinguishable PFGE patterns of ampicillin and tetracycline-resistant isolates in cattle and humans (Lupindu *et al.*, 2015). A cluster analysis of *E. coli* phylogroups found that human, pig, and chicken isolates clustered together (Jakobsen *et al.*, 2010). One extensive ecological study reported a significant correlation between the prevalence of resistance in human and livestock isolates, for both cephalosporins and fluoroquinolones (Vieira *et al.*, 2011).

Thirteen studies suggested there was evidence of overlap of AMR determinants in human and food animal isolates. Of the 13 studies, one study based on WGS and plasmid reconstruction found that clonally unrelated human and poultry isolates carried ESBL genes encoded on genetically identical plasmids (de Been *et al.*, 2014). Eleven studies found that unrelated human and food animal isolates shared identical AMR genes, integrons and plasmids (Oppegaard *et al.*, 2001; Winokur *et al.*, 2001; Ho *et al.*, 2009, 2010; Moodley and

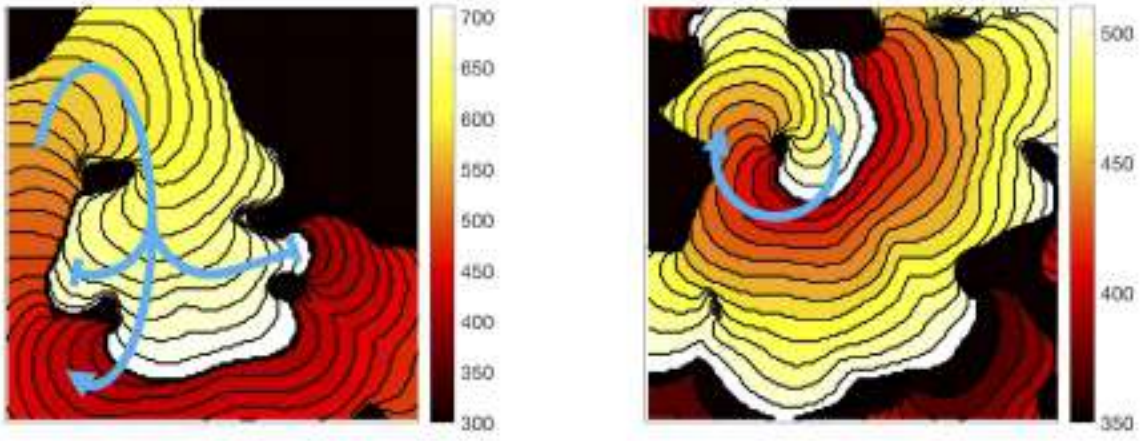


**FIGURE 9 |** Examples of sustained re-entry elicited by spiral wave initiation with the same pattern of heterogeneous diffusion at a length scale of 10 mm. **(A)** re-entry pathway with period of around 310 ms in simulated tissue with *CRNnormal* variant. **(B)** more compact re-entry pathway with much shorter period of around 130 ms in simulated tissue with *CRNremodelled* variant. Activation isochrones spaced at 10 ms intervals.

a uniform diffusion coefficient of 0.2 $mm^2ms^{-1}$, but larger length scales of 5.0 and 10.0 mm tended to produce a wider spread of activation delays.

- A delay in recovery relative to simulations with a uniform diffusion coefficient was found. This tended to be greater in simulations with heterogeneity on a smaller length scale, and greater with the *CRNnormal* variant rather than *CRNremodelled*.
- Distributions of APD tended to be positively skewed toward higher APD with the *CRNnormal* variant and negatively skewed toward lower APD with the *CRNremodelled* variant. This difference was attributed to inexcitable regions of simulated fibrosis acting as a current source during repolarization in simulations with the *CRNnormal* variant, and as a current sink in simulations with the *CRNremodelled* variant.
- With decremental pacing, simulations with smaller length scale heterogeneity and the *CRNremodelled* variant were most likely to result in sustained re-entry. However, the configuration of regions of simulated fibrosis also played an important role.
- With a spiral wave as an initial condition, simulations with smaller length scale heterogeneity and the *CRNremodelled* variant were also most likely to result in sustained re-entry.

The interaction of heterogenous diffusion, length scale, simulated fibrosis, and APD is complex and merits further investigation. The relationship of this study to previous work is discussed below.

## 4.1. Model of Fibrosis

The findings of the present study depend on the way that cellular electrophysiology and regions of fibrosis have been represented. In previous studies, regions of fibrosis have been represented in many different ways including inexcitable obstacles (Ten Tusscher and Panfilov, 2007), coupled elements with a fixed resting potential (Majumder et al., 2012), and with detailed fibroblast models (Sachse et al., 2009; Ashihara et al., 2012; Morgan et al., 2016; Zahid et al., 2016). The extent of coupling between fibroblasts and myocytes in the heart remains controversial because detailed experimental study of fibroblasts embedded in native cardiac tissue is difficult (Kohl and Gourdie, 2014), but novel experimental techniques have shown that non-myocytes undergo voltage excursions close to the border of scar tissue (Quinn et al., 2016). Regions of fibrosis have often been represented as areas of reduced tissue conductivity or a lower diffusion coefficient in computational studies (Gonzales et al., 2014; McDowell et al., 2015; Zahid et al., 2016).

In the present study regions of diffuse fibrosis were represented by smoothly varying but reduced diffusion, and focal fibrosis was represented as inexcitable tissue with a fixed diffusion coefficient of 0.05 $mm^2ms^{-1}$. The slowed upstroke and lower amplitude of voltage excursion observed in simulated fibrosed regions compared to normal tissue was comparable to other studies that have used more detailed models of fibroblast electrophysiology (Ashihara et al., 2012; Zahid et al., 2016) as well as experimental observations (Kohl and Gourdie, 2014). Nevertheless, further work with more detailed fibroblast models would be a valuable extension to the present study.

An additional set of simulations was done to compare the effect of simulations that used smoothly varying diffusion fields with simulations where the diffusion coefficient was set to 0.05 $mm^2ms^{-1}$ in fibrosed regions and 0.2 $mm^2ms^{-1}$ elsewhere (see **Supplementary Figure A**). With the *CRNnormal* variant, simulations with abrupt changes in diffusion had a longer APD and greater APD dispersion, especially at shorter length scales, compared to simulations with smoothly varying diffusion. With both variants, the delay in activation time was much shorter compared to simulations with smoothly varying diffusion. The overall response to decremental pacing was also similar for

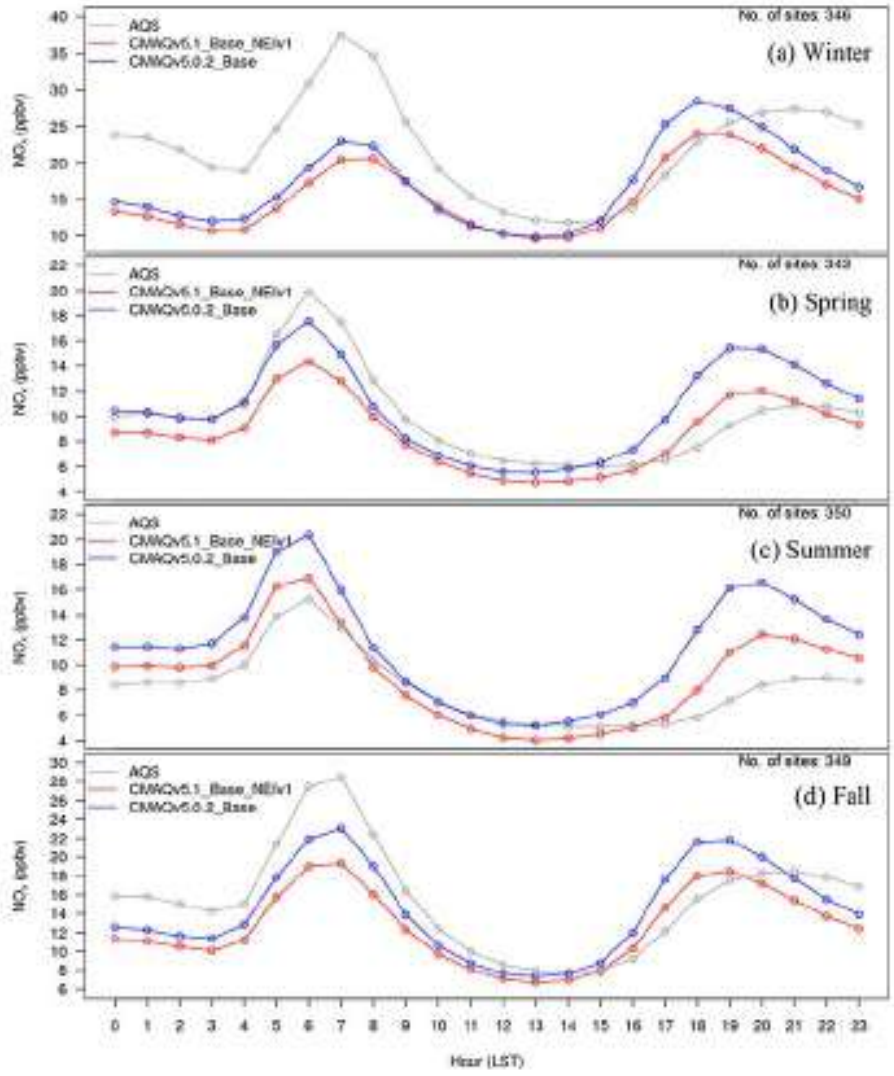


**Figure 15.**

Diurnal time series of seasonal $NO_x$ (ppbv) for AQS observations (gray), CMAQv5.0.2_Base simulation (blue) and CMAQv5.1_Base_NEIv1 simulation (red) for **(a)** winter, **(b)** spring, **(c)** summer and **(d)** fall.

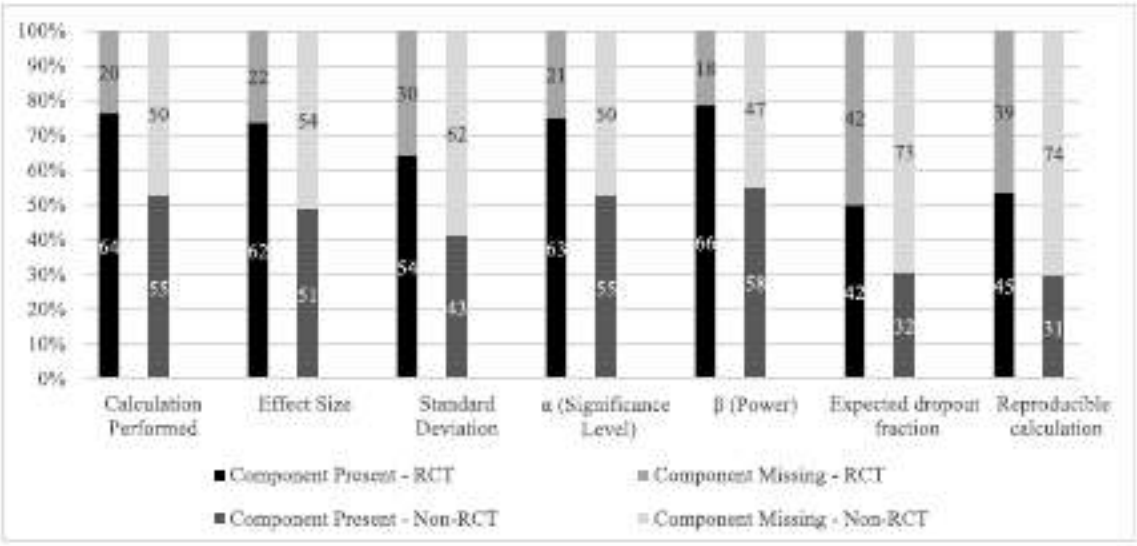


**Fig. 2.** Reported components of sample size calculation.
Frequencies of reported components of sample size calculation. The numbers in the columns represent the total number, whereas the Y-axis indicates the percentage. The first, darker column in the pairs represents the RCT, whereas the lighter second in the pairs represents the non-RCTs.

(score increase by 0.78, 95% CI 0.08–1.48, p = 0.030), and studies funded by foundations vs. studies with no funding (score increase by 1.39, 95% CI 0.47–2.31, p = 0.003) were associated with a higher score of SSCCCS.

## 4. Discussion

RCT protocols submitted to the Scientific Ethics Committees of The Capitol Region of Denmark were more inclined to include a sample size calculation compared to other study designs. This may be explained by the consensus that research trials including treatments or interventions should be conducted more carefully since the subjects potentially are at a greater risk compared to other study types. An increasing number of projected sick participants in the study also increased the likelihood of including a sample size calculation in the protocol, possibly also explained by the greater respect when the study involves treatment.

Studies funded by a foundation included a sample size calculation more often than studies funded by other means and studies not funded. More strict foundation regulations possibly explain this. Also, investigators pursuing funding with major funding bodies likely pay more attention to important details of their study's design, and consequently studies including realistic and scientifically sound considerations about projected sample size are more likely to obtain funding.

Interestingly, more sample size calculations were performed in newer studies (from 2013 through 2015). This could be explained by more awareness in general among researchers about power and sample size in scientific studies as time passes.

Our study has several strengths: the consecutive inclusion of study protocols during a specified time period led to a random pattern of study characteristics in our sample thus reducing bias. The wide variety of project-specific explanatory variables included increased the information extracted from this study. The centralised structure of the Danish scientific ethics committees ensured a complete coverage of protocols since no local institutional review boards exist. The single, homogenous protocol report formula proved to be an easy way to standardize data, which if multiple formulae types were involved could induce confusion and misunderstanding. Conversely, it is a limitation of the study that it only included a small sample of protocols in a limited geographical area.

Ideally, planning of all studies with quantitative analysis involving human subjects should include a sample size estimation [7]. However, some study designs make sample size calculations difficult, specifically

**Table 2**
Characteristics of study protocols with missing sample size calculation.

| | RCT | | Descriptive | | Experimental | | Analytical | | Secondary data analysis | | Total | |
|---|---|---|---|---|---|---|---|---|---|---|---|---|
| | N = 16 | | N = 18 | | N = 13 | | N = 20 | | N = 5 | | N = 72 | |
| Researcher's reason for not including a sample size calculation in the protocol | | | | | | | | | | | | |
| Explorative study, N (%) | 12 | (60.0) | 7 | (38.9) | 6 | (46.2) | 6 | (37.5) | 2 | (40.0) | 33 | (45.8) |
| Incalculable design, N (%) | 3 | (15.0) | 4 | (22.2) | 2 | (15.4) | 3 | (18.8) | 0 | (0.0) | 12 | (16.7) |
| Calculated prior or later, N (%) | 1 | (5.0) | 3 | (16.7) | 4 | (30.8) | 6 | (37.5) | 3 | (60.0) | 17 | (23.6) |
| None, N (%) | 4 | (20.0) | 4 | (22.2) | 1 | (7.7) | 1 | (6.3) | 0 | (0.0) | 10 | (13.9) |
| Researcher's sample size rationale | | | | | | | | | | | | |
| Similar studies, N (%) | 5 | (25.0) | 0 | (0.0) | 1 | (7.7) | 3 | (18.8) | 0 | (0.0) | 9 | (12.5) |
| Experience, N (%) | 1 | (5.0) | 9 | (50.0) | 5 | (38.5) | 5 | (31.3) | 3 | (60.0) | 23 | (31.9) |
| Predetermined size, N (%) | 1 | (5.0) | 1 | (5.6) | 2 | (15.4) | 2 | (12.5) | 1 | (20.0) | 7 | (9.7) |
| Calculated prior or later, N (%) | 3 | (15.0) | 3 | (16.7) | 1 | (7.7) | 1 | (6.3) | 0 | (0.0) | 8 | (11.1) |
| None, N (%) | 10 | (50.0) | 5 | (27.8) | 4 | (30.8) | 5 | (31.3) | 1 | (20.0) | 25 | (34.7) |

When sample size was estimated without a calculation, the reason for missing calculation (values: missing data/pilot study/incalculable design/calculated prior or later/none) and the sample size rationale (values: similar studies/experience/predetermined size/calculated prior or later/none) were found in the statistical subsection of the protocol.
Explorative study: some constant or variable (e.g. SD) is unknown, often not specified which in the protocol.
Incalculable design: the sample size calculation deemed "incalculable" by the investigator due to the study design.

**TABLE 1** Oligonucleotide primers used for amplification of SLA genes

| Gene | Orientation | Sequence (5′-) | CDNA position | Domain |
|---|---|---|---|---|
| SLA-1,-2, -3, -7, and -8 | Sense | GACACGCAGTTCGTGHGGTTC | 153-163 | α1 |
| SLA-6 | Sense | AGGACCCGCGTCTGGAGAAG | 150 | α1 |
| SLA-1,-2,-3,-6, -7, and -8 | Anti-sense | CTGGAAGGTCCCATCCCCTG | 789-799 | α3 |
| SLA-1,-2,-3, -6, and -7 | Anti-sense | GCTGCACMTGGCAGGTGTAGC | 851-861 | α3 |
| SLA-DQA | Sense | GAGCGCCTGTGGAGGTGAAG | 54 | Leader |
| SLA-DQA | Sense | GACCATGTTGCCTCCTATGGC | 85 | α1 |
| SLA-DQA | Anti-sense | CAGATGAGGGTGTTGGGCTGAC | 398 | α2 |
| SLA-DQA | Anti-sense | GACAGAGTGCCCGTTCTTCAAC | 462 | α2 |
| SLA-DQB1 | Sense | GAGACTCTCCACAGGATTTCGTG | 98 | β1 |
| SLA-DQB1 | Anti-sense | ACTGTAGGTTGCACTCGCCG | 395 | β2 |
| SLA-DRB1 | Sense | GGGACAYCSCACMGCATTTC | 89 | β1 |
| SLA-DRB1 | Sense | GAGTGYCRTTTCTTCAVYGGGAC | 127 | β1 |
| SLA-DRB1 | Anti-sense | CAGAGCAGACCAGGAGGTTGTG | 421 | β2 |
| SLA-DRB1 | Anti-sense | GGTCCAGTCTCCATTAGGGATC | 552 | β2 |

Abbreviation: SLA, swine leukocyte antigen.

**TABLE 2** Classical MHC class I and class II genotypes of inbred Babraham pigs

| | SLA-1 | SLA-2 | SLA-3 | DRB1 | DQA | DQB1 |
|---|---|---|---|---|---|---|
| Sequencing | *14:02[a] | *11:04[b] | *04:03[c]/*04:02 | *05:01 | *01:03 | *08:01 or *08:02 |
| SSP typing | *14:02 | *11:04 | *04:XX | *05:XX | *01:XX | *08:XX |

Abbreviations: MHC, major histocompatibility complex; SLA, swine leukocyte antigen; SSP, sequence-specific typing primers.

[a] Previously known as *SLA-1*es11*.

[b] Previously known as *SLA-2*es22*.

[c] Previously known as *SLA-3*04es32*.

Both SSP typing and sequencing methods confirmed homozygosity at the *SLA-1*, *SLA-2*, *SLA-DQA*, *SLA-DRB1* and *SLA-DQB1* loci (Table 2). The sequenced region of *SLA-DQB1*, containing the majority of both beta domains, could not differentiate between alleles *SLA-DQB1*08:01* and *SLA-DQB1*08:02*, which differ from each other at two nucleotide positions outside of the sequenced region (ie, at positions +52 and +606). This gene was nevertheless identical over the sequenced region in all animals based on reads from eight clones per animal. Only three sequencing reads from two animals were recovered for *SLA-3*. One of these reads corresponded with *SLA-3*04:02* and the remaining two reads corresponded with *SLA-3*04:03*, indicating that at least one of the six animals is a heterozygote at this locus. These two alleles differ only in the alpha-3 domain, by both a 12-bp insertion in *SLA-3*04:03* and a single non-synonymous mutation 9 bp upstream of the insertion. However, it is uncertain what, if any, influence these differences have on peptide-binding and receptor interactions, especially as this region is distal from the peptide-binding regions of the alpha-1 and alpha-2 domains. The paucity of *SLA-3* reads is likely due to the co-amplification of *SLA-3* cDNA with *SLA-1* and *SLA-2*, both of which are considered more highly expressed.[17,18] The haplotype that corresponds to the genotype *SLA-1*14:02-SLA-3*04:03-SLA-2*11:04-DRB1*05:01-DQB1*08:01* has been previously designated by the ISAG/IUIS-VIC SLA Nomenclature Committee Hp-55.6. The class I haplotype Hp-55.0 was originally described in the ESK-4 cell line,[19] while the class II haplotype Hp-0.6 has been detected in several pig breeds including Yucatan,[20] Austrian Pietrain,[21] Chinese Bama miniature pigs,[22] as well as the SK-RST cell line.[19]

Sequencing reads were additionally obtained for the non-classical MHC class I genes (*SLA-6*, *SLA-7*, and *SLA-8*) due to broad primer specificity. A total of six identical reads from three animals were identified for *SLA-6*, all of which contained the intron between the first two alpha domains, and thus originated from either unspliced mRNA or contaminating genomic DNA. Despite this, both exons were in frame and putatively functional. All of these reads also differed by at least 4 bp from the nine known *SLA-6* alleles in IPD-MHC, with five alleles being equally close (*SLA-6*01:01*, *SLA-6*03:01*, *SLA-6*04:01*, *SLA-6*05:01* and *SLA-6*06:01*). Reads specific for *SLA-7* ($n = 1$) and *SLA-8* ($n = 8$, from four animals) were also detected, likely due to the degenerate nature of the *SLA-6* primers used for cDNA amplification. Only three alleles of *SLA-7* are currently described within the IPD-MHC database, and the closest of these, *SLA-7*01:01*, differs by 2 bp to the single read sequenced from the Babraham samples. For *SLA-8*, all of the sequencing reads were identical to each other and were also exact matches for known alleles *SLA-8*01:01*, *SLA-8*04:01* and *SLA-8*05:01*. As the sequenced reads did not span the entire transcript, it could not be ascertained which, if any, of